Supplementary Materials and Methods

Vascular staining and imaging

Following FITC-dextran/agarose casting, euthanized mice were placed on ice until casts set. For imaging and 3D reconstruction, line scans were recorded at 1 µm increments in the *z*-plane (total *z*-plane displacement 150-600 µm). For whole-mount BrdU imaging, *z*-stacks (0.5 µm increments) were captured.

Hypoxia assay

Briefly, mice were injected intraperitoneally with 60 mg/kg body weight pimonidazole HCl. After 90 minutes, mice were transcardially perfused with 1% PFA; brain tissue was harvested and prepared for cryosectioning. Immunostaining against 1:10 dilution of MAb1 (4.3.11.3 mouse IgG_1 anti-pimonidazole monoclonal antibody; HPI) was performed according to manufacturer's recommendations. VECTASHIELD Mounting Medium with DAPI (Vector Labs) was used. Images were captured using an upright fluorescence microscope (Leica) and SlideBook software.

Fig. S1. Rbpj was effectively deleted from ECs in *Cdh5(PAC)-CreER^{T2}; Rbpj$^{fx/fx}$* brains.

Rbpj immunohistochemistry following Rbpj$^{i\Delta EC}$ deletion. (A-B) TAM at P1, P2; harvest at P14. (C-D) Adult = TAM at 6 weeks; harvest at 12 weeks. Control EC nuclei (arrowheads in (A,C)) expressed Rbpj; Mutant EC nuclei (arrowheads in (B,D)) lacked Rbpj. For P14, N=4 controls, N=4 mutants. For adult, N=3 controls, N=3 mutants. Nuclei were counterstained with hematoxylin. Scale bars: 50 μm.

Fig. S2. Schematic of whole mount cortical preparation.

Cerebral cortex was sliced off with a scalpel and placed in PBS on a welled microscope slide. Coverslip was applied for imaging; for inverted imaging, PARAFILM held coverslip in place.

Fig. S3. Method for measuring diameters of AV connections.

(A-D) mGFP+ ECs are shown in whole mount cerebral cortex. (A) Capillaries (purple outline) lay between arteries/arterioles (a, red outline) and venules/veins (v, blue outline) in the control. (B) Enlarged AV connections (yellow outline) directly connected artery to vein in Rbpj$^{i\Delta EC}$ mice. To generate the graph in Fig. 1G, diameter was measured at a point along each AV connection, as shown in (C-D). Multiple AV connections were measured among multiple fields for each brain. (E-F) Because *Efnb2$^{tau\text{-}lacZ}$* staining showed a clear demarcation of: 1) the arterial vs. venous capillary segments in controls, and 2) the AV shunt/arteriole interface in mutants, we measured AV shunts on *Efnb2$^{tau\text{-}lacZ}$* stained control and mutant brains. Positions and values for measurements are shown. (G) Quantification of vessel diameters in (E-F). *P*=0.0066. N=4 controls (80 AV connections), N=4 mutants (52 AV connections). Scale bars: 100 μm.

Fig. S4. Endothelial deletion of Rbpj led to thinner smooth muscle cell layer in intestinal mesentery and increased pericyte coverage in intestinal submucosa at P14.

(A-B) Immunostaining against α-SMA revealed that the smooth muscle cell layer surrounding endothelium was thinner in sections through mutant intestinal mesentery. Quantified in (E, upper). *P*=0.0117. N=5 controls (40 arteries), N=5 mutants (29 arteries). (C-D) Immunostaining against CD13 indicated that pericyte coverage was increased in sections through intestinal submucosa. Quantified in (E, lower). *P*=0.0119. N=3 controls (30 fields), N=3 mutants (30 fields). Scale bars: (A-D) 50 μm. a, artery; v, vein.

Fig. S5. Endothelial deletion of Rbpj did not alter smooth muscle cell coverage or pericyte coverage in myocardium at P14.

(A-B) Immunostaining against α-SMA revealed that the smooth muscle cell layer surrounding endothelium was not altered in sections through myocardium. Quantified in (E). *P*=0.5158. N=3 controls (6 arteries), N=3 mutants (9 arteries). Immunostaining against CD13 indicated that pericyte coverage was not increased in sections through myocardium. Quantified in (F). *P*=0.1100. N=3 controls (30 fields), N=3 mutants (30 fields). Scale bars: (A-B) 200 μm; (C-D) 50 μm. a, artery; v, vein.

Movie 1. 3D reconstruction of ~100 μm Z-stack from P14 control cerebrovasculature using 2PEFM.

Movie 2. 3D reconstruction of ~100 μm Z-stack from P14 Rbpj$^{i\Delta EC}$ cerebrovasculature using 2PEFM.

Movie 3. 3D reconstruction of ~100 μm Z-stack from P14 control forebrain using 2PEFM.

Movie 4. 3D reconstruction of ~100 μm Z-stack from P14 Rbpj$^{i\Delta EC}$ forebrain using 2PEFM.

Movie 5. 3D reconstruction of ~100 µm Z-stack from P14 control cerebellum using 2PEFM.

Movie 6. 3D reconstruction of ~100 µm Z-stack from P14 Rbpj$^{i\Delta EC}$ cerebellum using 2PEFM.

Movie 7. Mice exhibited impaired gross motor coordination at P14 following deletion of endothelial Rbpj from birth.

Movie clip begins with a P14 control mouse on the left, and its Rbpj$^{i\Delta EC}$ littermate on the right. As compared to the control, the Rbpj$^{i\Delta EC}$ mouse was slow to initiate movement and walked unsteadily.

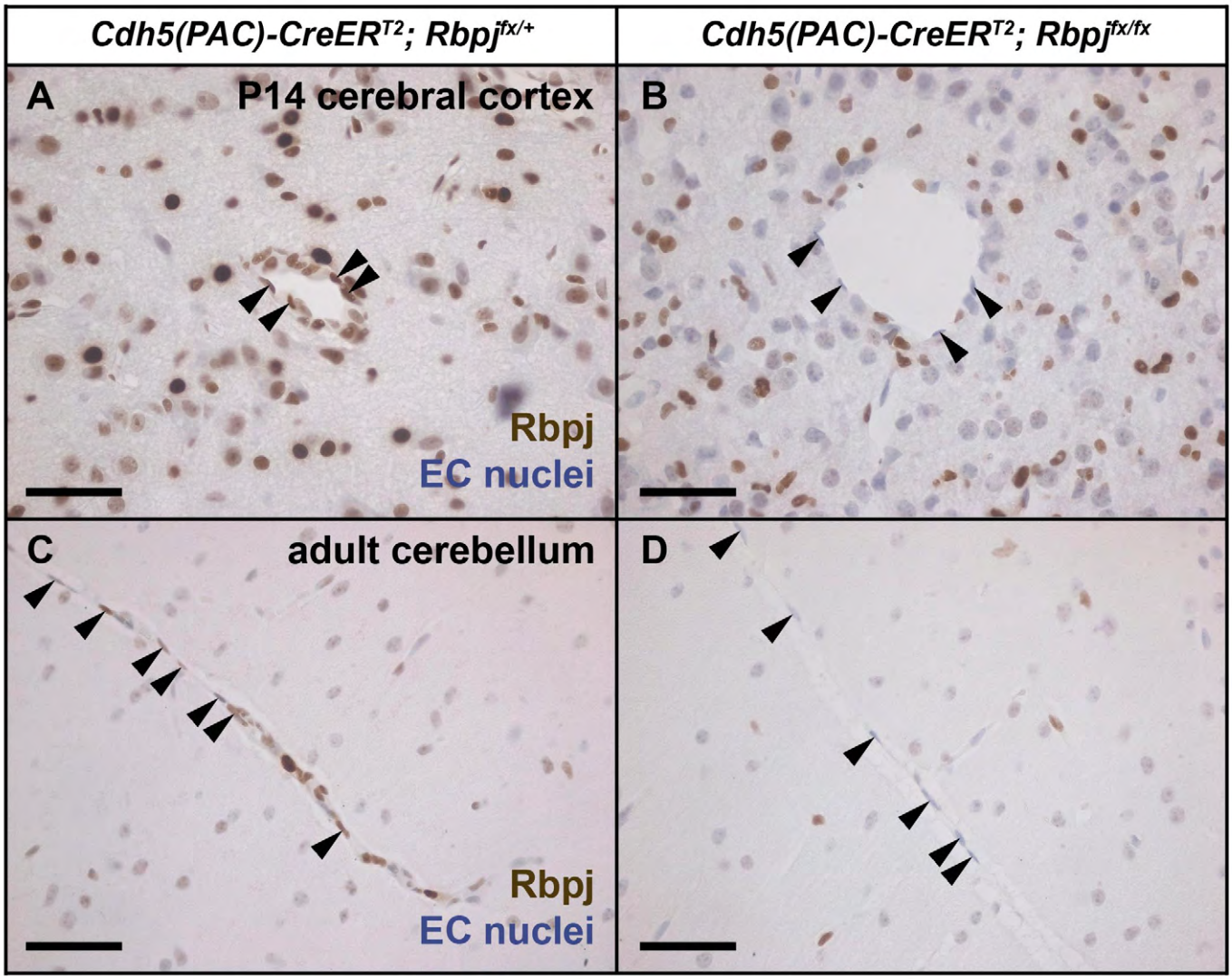
Cdh5(PAC)-CreER^{T2}; Rbpj$^{fx/+}$
Cdh5(PAC)-CreER^{T2}; Rbpj$^{fx/fx}$
A
P14 cerebral cortex
Rbpj
EC nuclei
B
C
adult cerebellum
Rbpj
EC nuclei
D

Figure S1

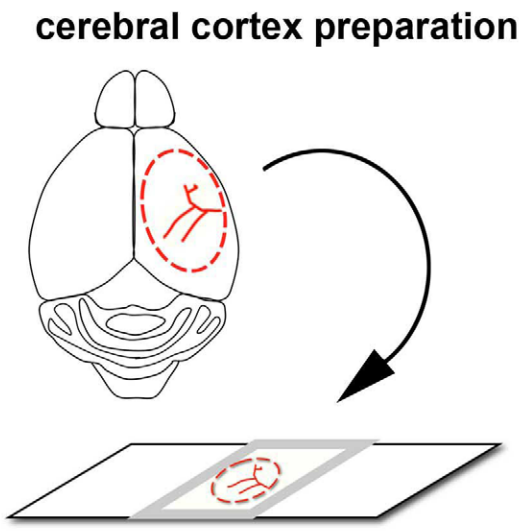

Figure S2

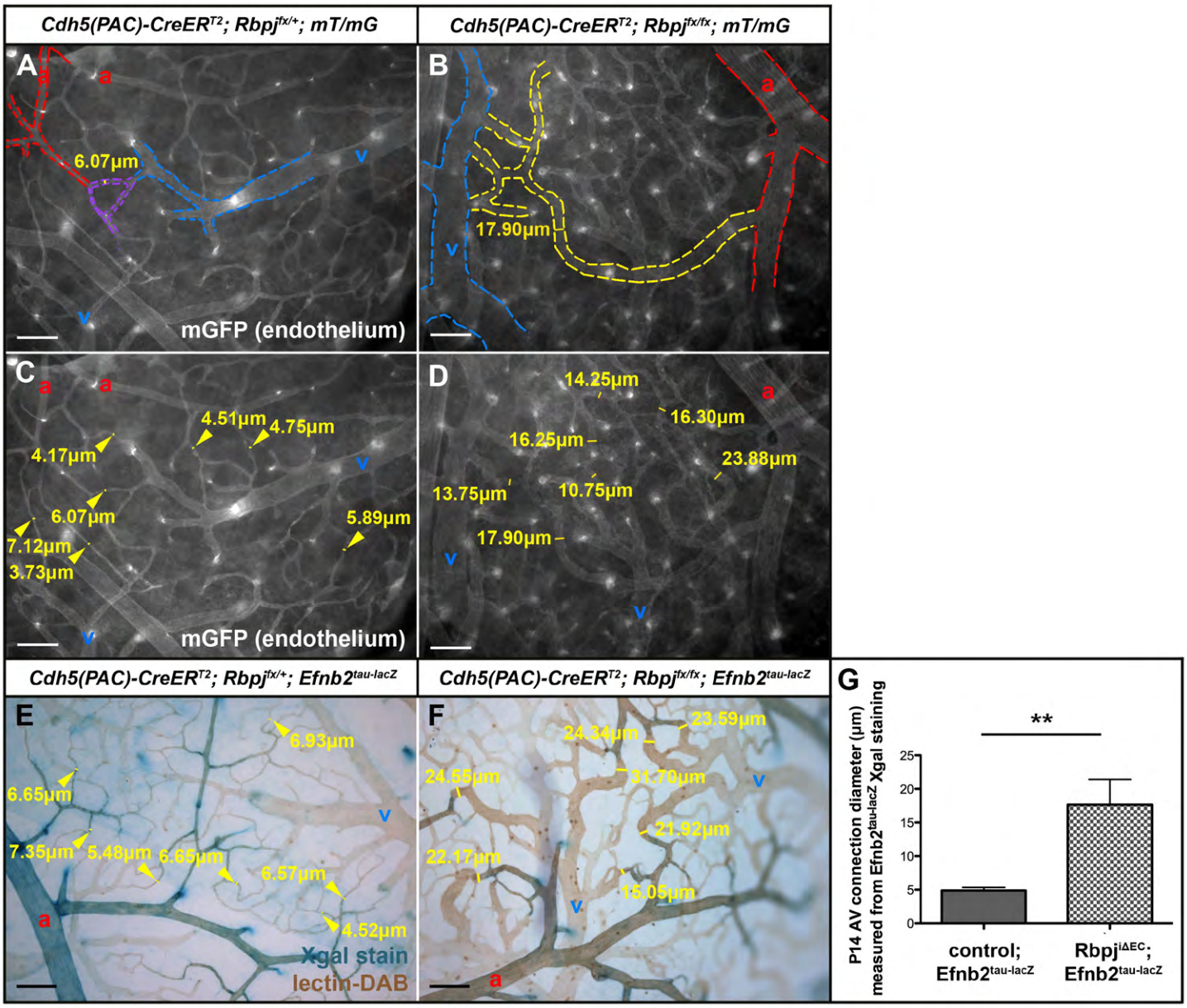
Cdh5(PAC)-CreER^{T2}; Rbpj$^{fx/+}$; mT/mG
Cdh5(PAC)-CreER^{T2}; Rbpj$^{fx/fx}$; mT/mG
A
B
C
D
a
v
6.07μm
17.90μm
mGFP (endothelium)
4.51μm
4.75μm
4.17μm
6.07μm
5.89μm
7.12μm
3.73μm
14.25μm
16.30μm
16.25μm
23.88μm
13.75μm
10.75μm
17.90μm
Cdh5(PAC)-CreER^{T2}; Rbpj$^{fx/+}$; Efnb2$^{tau-lacZ}$
Cdh5(PAC)-CreER^{T2}; Rbpj$^{fx/fx}$; Efnb2$^{tau-lacZ}$
E
F
6.93μm
6.65μm
7.35μm
5.48μm
6.65μm
6.57μm
4.52μm
Xgal stain
lectin-DAB
24.34μm
23.59μm
24.55μm
31.70μm
21.92μm
22.17μm
15.05μm
G
P14 AV connection diameter (μm) measured from Efnb2$^{tau-lacZ}$ Xgal staining
**
25
20
15
10
5
0
control; Efnb2$^{tau-lacZ}$
Rbpj^{iΔEC}; Efnb2$^{tau-lacZ}$

Figure S3

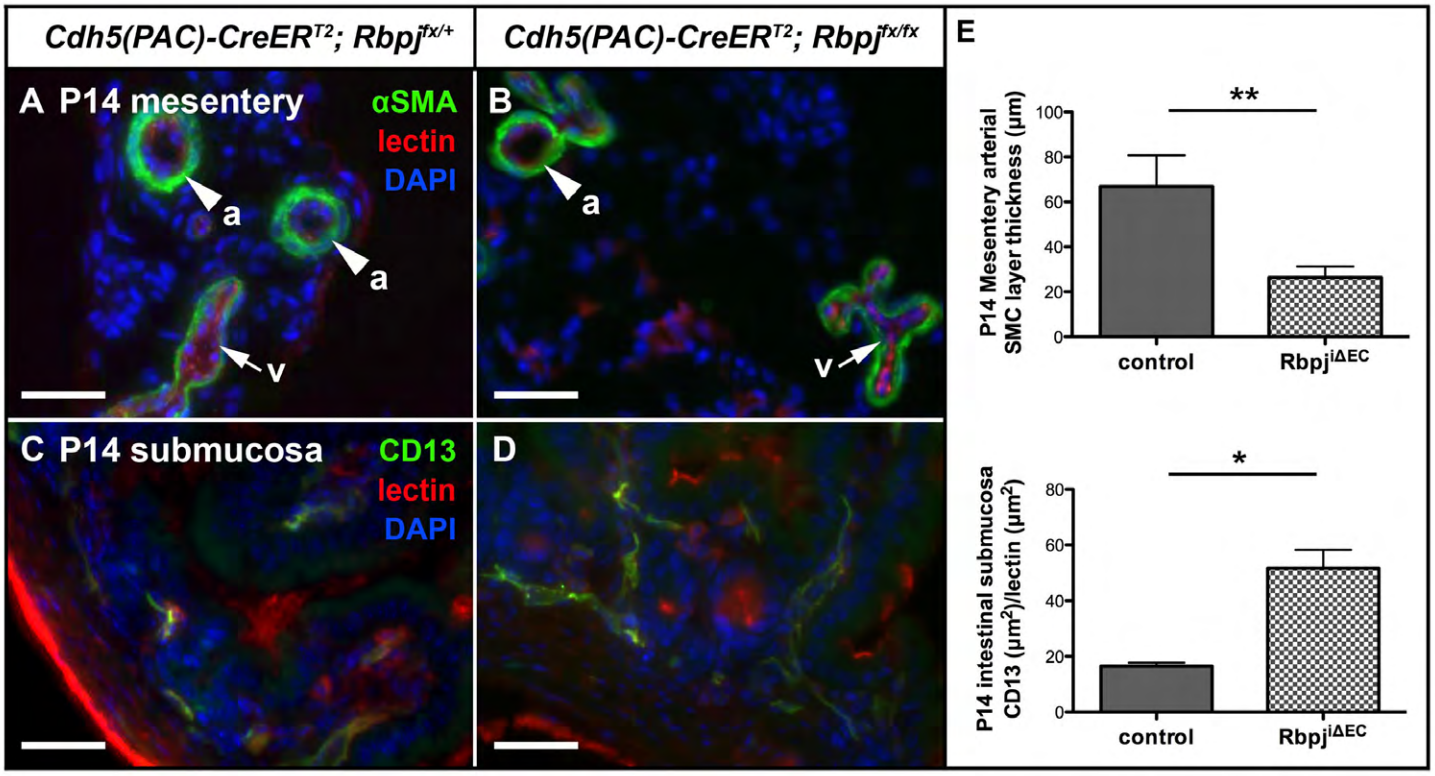
Cdh5(PAC)-CreER^{T2}; Rbpj$^{fx/+}$
Cdh5(PAC)-CreER^{T2}; Rbpj$^{fx/fx}$
A P14 mesentery
αSMA
lectin
DAPI
a
a
v
B
a
v
C P14 submucosa
CD13
lectin
DAPI
D
E
P14 Mesentery arterial SMC layer thickness (μm)
100
80
60
40
20
0
**
control
Rbpj^{iΔEC}
P14 intestinal submucosa CD13 (μm^2)/lectin (μm^2)
80
60
40
20
0
*
control
Rbpj^{iΔEC}

Figure S4

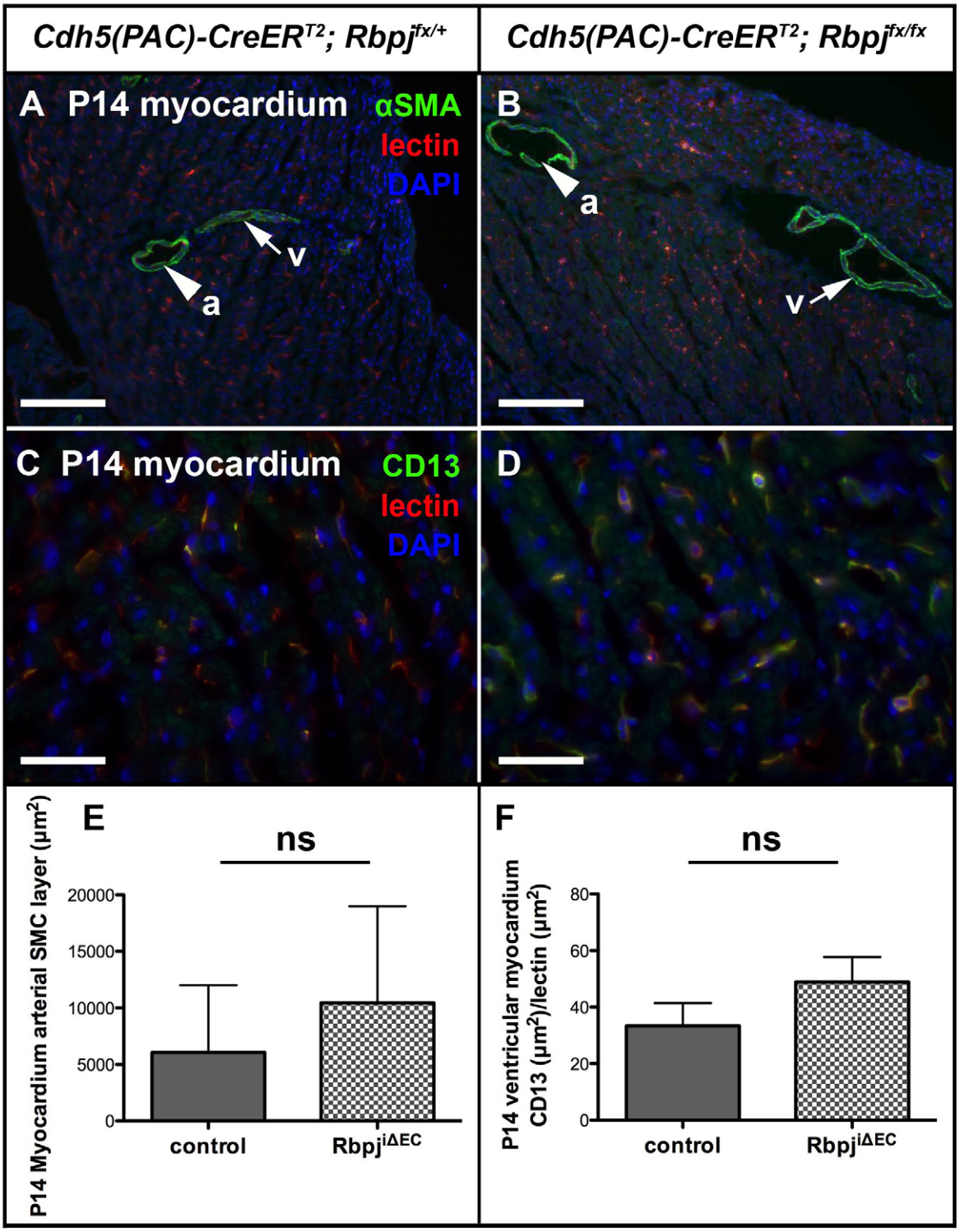
Cdh5(PAC)-CreER^{T2}; Rbpj$^{fx/+}$
Cdh5(PAC)-CreER^{T2}; Rbpj$^{fx/fx}$
A P14 myocardium
αSMA
lectin
DAPI
a
v
B
a
v
C P14 myocardium
CD13
lectin
DAPI
D
E
ns
P14 Myocardium arterial SMC layer (µm^2)
20000
15000
10000
5000
0
control
Rbpj^{iΔEC}
F
ns
P14 ventricular myocardium CD13 (µm^2)/lectin (µm^2)
80
60
40
20
0
control
Rbpj^{iΔEC}

Figure S5

Movie 1.

Movie 2.

Movie 3.

Movie 4.

Movie 5.

Movie 6.

Movie 7.

Table S1. Primers used for quantitative RT-PCR

Mouse gene	Direction	Primer sequence
Cdh5	forward	CGCCAAAAGAGAGACTGGAT
	reverse	CGTTGGACTTGATCTTTCCC
Efnb2	forward	TCTTTGGAGGGCCTGGATAAC
	reverse	CATCTCCTGCACGATGTACAC
Ephb4	forward	CCTCTGATCCCACCTACACAA
	reverse	ATGACCTCCCACATGACGA
Hey1	forward	CTTGCAGATGACCGTGGA
	reverse	GTGAGGCATTCCCGAAAC
Hey2	forward	TGAAGATGCTCCAGGCTACA
	reverse	CACTCTCGGAATCCAATGCT
Pai1	forward	GCTGGTGAATGCCCTCTAC
	reverse	GGCAGCCTGGTCATGTTG
Rasa1	forward	TCCTTAGTCAGACAAATGTTGTCAAT
	reverse	AAACAAGAAACGTGACTGTAATAACC
Smad4	forward	GGAATAGCTCCAGCCATCAG
	reverse	AGCCCTTCACAAAGCTCATC
Tgfb1	forward	TGACGTCACTGGAGTTGTACGG
	reverse	GGTTCATGTCATGGATGGTGC
Vegfa	forward	ACGTACTTGCAGATGTGACAAGCC
	reverse	AAGTGCTCCTCGAAGAGTCTCCT